Carbohydrate Polymers 104 (2014) 213–222

Contents lists available at ScienceDirect

Carbohydrate Polymers

journal homepage: www.elsevier.com/locate/carbpol

Complex microparticulate systems based on glycidyl methacrylate and xanthan

Maria-Andreea Lungan[a], Marcel Popa[a], Jacques Desbrieres[b], Stefania Racovita[c], Silvia Vasiliu[c,*]

[a] "Gheorghe Asachi" Technical University of Iasi, Faculty of Chemical Engineering and Environmental Protection, Department of Natural and Synthetic Polymers, Prof. dr. docent Dimitrie Mangeron Street, No. 73, 700050 Iasi, Romania
[b] Pau and Pays de l'Adour University (UPPA), Institut des Sciences Analytiques et de Physico-Chimie pour l'Environnement et les Materiaux (IPREM/EPCP), UMR CNRS 5254, Helioparc Pau Pyrenees, 2, av. President Angot, 64053 Pau Cedex 09, France
[c] "Petru Poni" Institute of Macromolecular Chemistry, Grigore Ghica Voda Alley No. 41A, 700487 Iasi, Romania

ARTICLE INFO

Article history:
Received 18 October 2013
Received in revised form 8 January 2014
Accepted 11 January 2014
Available online 21 January 2014

Keywords:
Glycidyl methacrylate
Xanthan gum
Suspension polymerization
Surface area
Porous microparticles

ABSTRACT

Porous microparticles based on glycidyl methacrylate, dimethacrylic monomers [ethylene glycol dimethacrylate, diethylene glycol dimethacrylate, triethylene glycol dimethacrylate] and xanthan gum were synthesized by aqueous suspension polymerization method in the presence of toluene as diluent using two types of initiators: benzoyl peroxide and ammonium persulfate. The G microparticles based on glycidyl methacrylate and dimethacrylic monomers and X microparticles based on glycidyl methacrylate, xanthan and dimethacrylic monomers were characterized by various techniques including FT-IR spectroscopy, TG analysis, SEM analysis and DVS method. The specific surface areas were determined by DVS method, while the copolymer porosities and pore volume were obtained from the apparent and skeletal densities. The results have indicated that xanthan was included in the crosslinked matrix by means of covalent bonds. X microparticles have a porous structure with higher specific surface area (129–44 m^2/g) and higher sorption capacities compared with G microparticles (69–31 m^2/g).

1. Introduction

The selection, modification and elaboration of new materials for various applications are important criteria in the development of human civilization. Nowadays polymeric materials play an essential role in every field of human activities, taking part more and more in all the aspects of our daily existence. The increased interest of the scientific community for the polymeric microparticles is due to their properties as well as of the various requirements of medical and pharmaceutical fields.

Glycidyl methacrylate (GMA) is an attractive vinyl monomer because of its low toxicity, lower cost compared with other acrylic monomers, versatile properties and especially due to the presence in its molecule of two functional groups such as epoxy and acrylic groups, respectively (Jin, Lee, Ha, Lee, & Choe, 2007; Rahman et al., 2012).

Since the pioneering work of Svec, Hradil, Coupek, and Kalai (1975) on macroporous copolymer based on GMA and ethylene glycol dimethacrylate (EGDMA) a large number of papers have been focused on more detailed studies of the synthesis, properties, chemical modification and applications of copolymers based on GMA. Applications area of these types of copolymers is quite large, they being used as chelating ion exchangers (Malovic et al., 2007; Senkal & Yavuz, 2006), macromolecular supports for enzyme immobilization (Bencina, Bencina, Stancar, & Podgornik, 2005; Miletic, Rohandi, Vukovic, Nastasovic, & Loos, 2009; Milosavic, Prodanovic, Joranovic, & Vujcic, 2007; Vaidya, Ingavle, Ponrathnam, Kulkarni, & Nene, 2008) or adsorbents for blood detoxification (Danquah, Ho, & Forde, 2007). In literature are presented various methods to prepare porous microparticles based on GMA such as suspension polymerization (Qi et al., 2002), seeded polymerization (Kim & Suh, 2008), precipitation polymerization (Jiang & Tu, 2010), surfactant reverse micelles swelling methods (Zhou, Gu, Su, & Ma, 2007), dispersion polymerization and membrane emulsification polymerization (Wang, Zhang, Ma, & Su, 2006). Among these methods the suspension polymerization is one of the most common techniques used for the preparation of porous microparticles due to some advantages, such as: (a) small number of reagents in comparison with emulsion polymerization or other techniques; (b) lower cost compared to a broad spectrum of properties acquired by the microparticles; (c) excellent heat transfer during the process; (d) ability to control the size and size distribution of microparticles; (e) simple purification

* Corresponding author. Tel.: +40 232 217454; fax: +40 232 211299.
E-mail addresses: maria_andreea.lungan@yahoo.com (M.-A. Lungan), marpopa2001@yahoo.fr (M. Popa), jacques.desbrieres@univ-pau.fr (J. Desbrieres), stefania.racovita@icmpp.ro (S. Racovita), msilvia@icmpp.ro (S. Vasiliu).

0144-8617/$ – see front matter © 2014 Elsevier Ltd. All rights reserved.
http://dx.doi.org/10.1016/j.carbpol.2014.01.035

method for the final product (Brooks, 2010; Vivaldo-Lima, Wood, Hamielec, & Penlidis, 1997).

In suspension polymerization technique, the polymerization mixture should be adjusted according to the required properties of microparticles, especially for the achievement of the spherical shape, size and porosity. Thus, for the separation of small molecules or oligomers are used microparticles with small pores and a narrow pore distribution while for protein separation are needed porous systems which have pores with large diameters. It is known that the porosity of the copolymers is controlled by the following parameters: crosslinker and monomer concentrations, type and molar ratio of the monomers, amount and type of porogenic agent used and polymerization temperature (Malik, Ali, & Waseem, 2006; Okay, 2000). For medical applications it is very important to improve the biocompatibility and to reduce the toxicity of the macromolecular supports. A combination between synthetic and natural polymers could lead to new polymeric materials with specific properties that can be used as supports for immobilization of various biologically active molecules (Vasiliu, Bunia, & Neagu, 2009). For this purpose, the present manuscript describes a new way for the synthesis of porous microparticles based on GMA and xanthan (XAN) using the suspension polymerization technique. Xanthan gum is an anionic polysaccharide produced by *Xanthomonas campestris* and due to its nature can provide remarkable properties to the new polymeric materials in terms of lack of toxicity and good biocompatibility. In the future studies we shall continue to explore the applications of these systems as macromolecular supports for immobilization of biologically active molecules in drug delivery and biotechnological fields.

2. Experimental

2.1. Materials

Glycidyl methacrylate (Sigma–Aldrich) was distilled under reduced pressure to remove the inhibitor. Ethylene glycol dimethacrylate, diethylene glycol dimethacrylate (DEGDMA), triethylene glycol dimethacrylate (TEGDMA) and xanthan gum were purchased from Sigma–Aldrich and were used as received.

All other reagents were of analytical grade and were purchased from Sigma–Aldrich. Benzoyl peroxide (BOP) and ammonium persulfate (APS) were used as initiators, while toluene was used as porogenic agent. Poly(vinyl alcohol) (PVA, M_w = 51.000 g/mol, degree of hydrolysis, 88%) was used as stabilizer. Ultra pure grade water was used in all experiments and has been prepared by purifying deionized water ($\Omega < 10^{-6}$ S/cm) with Millipore Simplicity-UV apparatus.

2.2. Preparation of copolymer microparticles

2.2.1. Synthesis of G microparticles

The microparticles based on GMA-EGDMA, GMA-DEGDMA and GMA-TEGDMA labeled G microparticles were prepared by aqueous suspension polymerization in a cylindrical reactor with a volume of 500 cm^3. The reaction mixture consists of two phases:

a) Aqueous phase consisting of distilled water as a dispersion medium and 1.5 wt.% PVA as suspension stabilizer.
b) Organic phase consisting of GMA (90 mol%), crosslinking agents [EGDMA (10% and 20% mol, respectively), DEGDMA (10 mol%), TEGDMA(10 mol%)], free radical initiator (BOP) (2.5 wt.% with respect to the total amount of the monomers) and toluene as porogenic agent [D = 0.5, where D = ml toluene/(ml toluene + ml monomers)]. The inert porogenic agent must be soluble in the monomer mixture but insoluble in the continuous phase of suspension polymerization.

2.2.2. Synthesis of X microparticles

The microparticles based on GMA-EGDMA-XAN, GMA-DEGDMA-XAN and GMA-TEGDMA-XAN, labeled X microparticles were obtained through the same procedure with few modifications:

1. The aqueous phase was formed by a solution of PAV and xanthan (1.5 wt.%).
2. In the aqueous phase a second free radical initiator (APS) is used to create radicals on polysaccharide chains. The XAN/monomers ratio was 1:23 (w/w) and (BOP + APS) content was 2.5 wt.% with respect to the total amount of monomers.

For all experiments the organic/aqueous phase ratio was 1:9. The copolymerization reactions were conducted under N_2 atmosphere for 8 h at 78 °C and 1 h at 90 °C with a stirring rate of 360 r.p.m.

Both sets of copolymers with and without XAN obtained in beaded form were separated by decantation, washed with hot water and then were extracted with methanol in a Soxhlet apparatus in order to remove traces of residual monomers and porogenic agent.

Finally, the G and X microparticles were dried under vacuum at 50 °C for 48 h and sieved.

2.3. Characterization of microparticles

The epoxy group content was determined by titrimetric method namely HCl-dioxane method (Vogel, 1958, Chapter XXXVIII). Simultaneously, epoxy group content in the structure of copolymers was determined by FT-IR analysis on the basis of a calibration curve using the peak areas at 908 cm^{-1} and 1717 cm^{-1} (Bakhshi, Zohuriaan-Mehr, Bouhendi, & Kabiri, 2009; Canto & Pessan, 2002).

FT-IR spectra were obtained on a Bruker Vertex FT-IR Spectrometer, resolution 2 cm^{-1}, in the range of 4000–400 cm^{-1}. In order to obtain the FT-IR spectra, a known quantity of microparticles (0.03 g) was mixed and ground with potassium bromide.

The thermal degradation of microparticles was performed in a METTLER 851 Derivatograph, carried out using 4 mg of sample and heated at a rate of 10 °C/min under nitrogen atmosphere. The weight loss versus temperature was recorded.

The number average diameter (D_n) and the particle size distribution of G and X microparticles were achieved using the principle of laser diffraction (Laser Diffraction Particle Size Analyzer WingSALD 7001).

The specific surface area of the microparticles was determined using the Brunauer, Emmet and Teller (BET) method (Ng & Mintova, 2008) using the fully automated gravimetric analyzer IGAsorp produced by Hiden Analytical, Warrington (UK).

The apparent (ρ_{ap}) and skeletal (ρ_{sp}) densities of microparticles were measured by pycnometric methods with mercury and heptane, respectively (Seidl, Malinsky, Dusek, & Heitz, 1967; Vlad & Vasiliu, 2010). The pore volume (PV) and the porosity (P) of microparticles were calculated as follows:

$$\mathrm{PV}\ \ (\mathrm{mL/g}) = \frac{1}{\rho_{ap}} - \frac{1}{\rho_{sp}} \tag{1}$$

$$\%P = 100 \cdot \left(1 - \frac{\rho_{ap}}{\rho_{sp}}\right) \tag{2}$$

Sorption–desorption isotherms were registered with fully automated gravimetric analyzer IGAsorp produced by Hiden Analytical, Warrington (UK). The weight change was measured with an

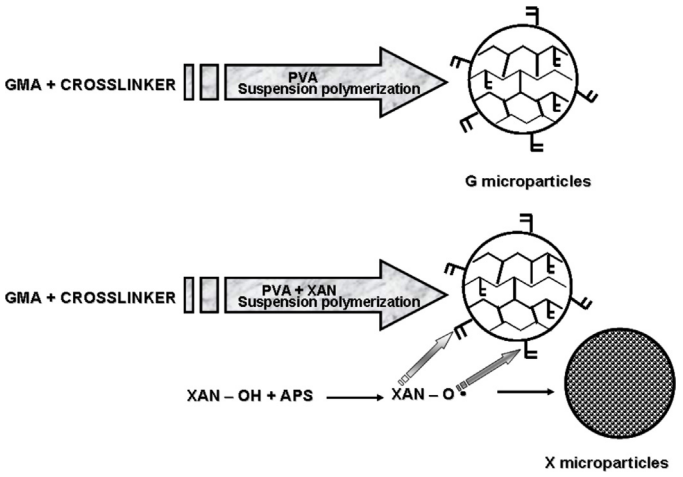

Scheme 1. Schematic representation of G and X microparticles synthesis.

ultrasensitive microbalance, system measurements being fully automated and controlled by a software package. The samples were dried at 25 °C in flowing nitrogen (250 mL/min.) until the equilibrium was reached (relative humidity (RH) < 1%). Then, RH was gradually increased from 0 to 90% and the sorption curves were registered. Desorption curves are obtained when RH was decreased.

The shape and the surface morphology of the G and X microparticles were observed using an Environmental Scanning Electron Microscope type Quanta 200 at 25 kV.

The yield of copolymerization was determined gravimetrically.

3. Results and discussion

3.1. Preparation of G and X microparticles

Porous G and X microparticles were synthesized by suspension polymerization technique. In Table 1 are presented the chemical structures of monomers, natural polymer, G and X microparticles.

The schematic representation of the synthesis of G and X microparticles is shown in Scheme 1.

As can be seen from Scheme 1 for the preparation of X microparticles is used a second initiator (APS) which determines the appearance of an active center on xanthan macromolecules. This macroradical can either attack the unreacted double bonds of the monomers or can react with the other macroradicals that are present in the reaction medium, leading to the formation of a new crosslinked polymer matrix in which the polysaccharide is linked by covalent bonds. The sample codes, composition and yields of copolymerization of the microparticles used in this study are presented in Table 2.

3.2. Characterization of the microparticles

3.2.1. FT-IR spectra

The FT-IR spectroscopy is an important tool in the elucidation of the structural clues being an easy way to detect the presence of chemical functional groups in the sample. The FT-IR spectra of XAN and GMA-EGDMA are well known in literature (Marinovic, Vukovic, Nastasovic, Milutinovic-Nikolic, & Jovanovic, 2011; Vasiliu, Bunia, Racovita, & Neagu, 2011). Fig. 1 shows the FT-IR spectra of X_2 microparticles, G_2 microparticles and XAN.

The spectrum of XAN presents peak at 3435 cm^{-1} that represent O—H asymmetric stretching vibrations. The peak representing >CH— stretching vibrations of $>CH_2$ group appears at 2920 cm^{-1}. The >C═O stretching of acetyl group appeared at 1737 cm^{-1} and

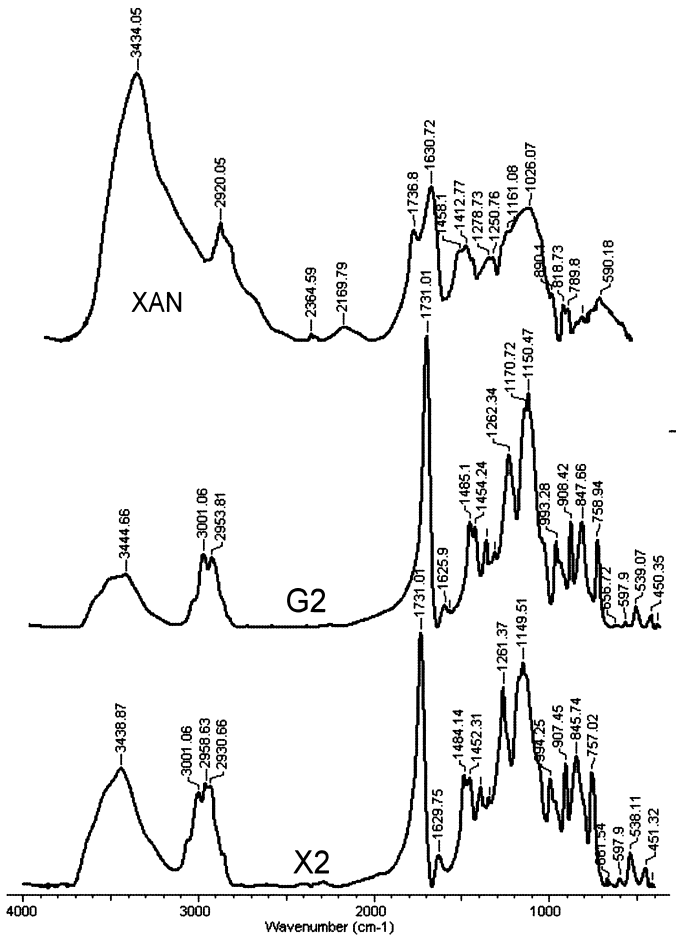

Fig. 1. FT-IR spectra of X_2 microparticles, G_2 microparticles and XAN.

the adsorption bands at 1631 cm^{-1} and 1413 cm^{-1} are due to the ν_s (COO^-) and ν_{as}(COO^-) from pyruvate and glucuronate groups.

In the spectrum of the G_2 microparticles the characteristic absorption bands were assigned as follows: the bands at 3001 and 2954 cm^{-1} correspond to the >CH— stretching vibrations; ester group vibrations appear at 1731 cm^{-1} [ν(C═O)] and at 1262 and 1150 cm^{-1} [ν(C—O)]; the bands at 1485 and 1454 cm^{-1} indicate the presence of the methylene groups; the band at 908 cm^{-1} corresponds to the epoxy ring vibrations. In case of X_2 microparticles is observed a slight shift of most absorption bands. This behavior is common for all types of X microparticles compared to G microparticles.

In general the specific bands of the starting polymers are overlapped and therefore to better highlight the differences between G and X microparticles the area of some characteristic bands was determined (Table 3).

From the analysis of the data from Table 3 it could be drawn the following conclusions:

- for all samples the peak areas of X microparticles are higher than those for G microparticles;
- the peak areas at 1150 cm^{-1} (C—O stretching vibration) of physical mixtures and G microparticles show approximately the same values because between them there is no chemical interaction;
- the increase of the peak area value at 1150 cm^{-1} for X microparticles compared with those for G microparticles and physical mixtures can be explained by the appearance of the new ether linkage demonstrating that xanthan reacts with the acrylic

Table 1
Chemical structure of monomers, natural polymer, G and X microparticles.

Monomers and polymers	Chemical structures
Glycidyl methacrylate	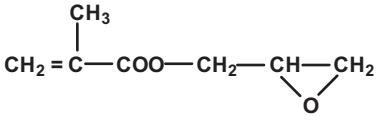
Dimethacrylic monomers	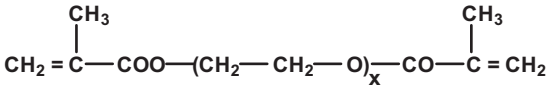
Xanthan gum (XAN-OH)	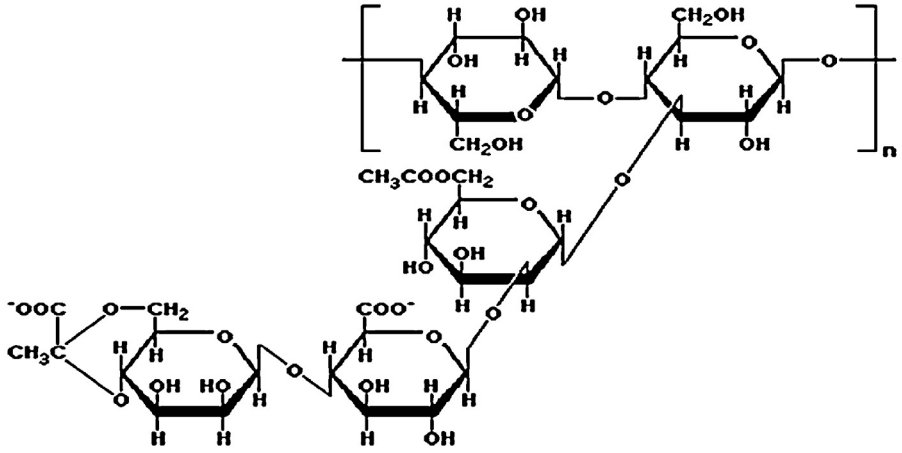
G microparticles	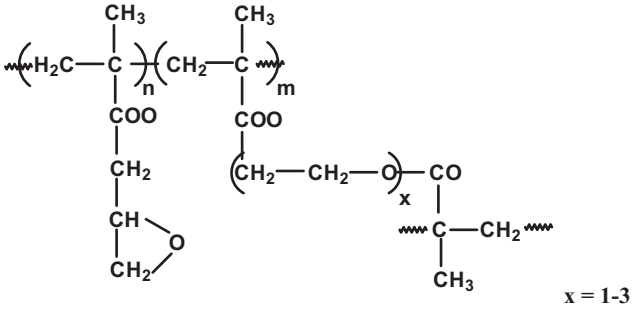 x = 1-3
X microparticles	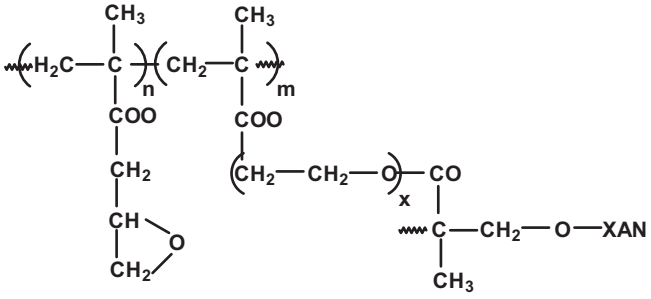

Table 2
Sample codes, composition and yield of copolymerization of G and X microparticles.

Sample codes	Crosslinker	GMA/crosslinker ratio (mol/mol)	Monomers/XAN ratio (w/w)	D (μm)	Yield of copolymerization (%)
G_1	EGDMA	90/10	–	316	94
G_2	EGDMA	80/20	–	243	93
G_3	DEGDMA	90/10	–	268	90
G_4	TEGDMA	90/10	–	252	85
X_1	EGDMA	90/10	23/1	179	98
X_2	EGDMA	80/20	23/1	150	95
X_3	DEGDMA	90/10	23/1	159	92
X_4	TEGDMA	90/10	23/1	160	87

Table 3
Areas of characteristic bands of X microparticles, G microparticles and physical mixture.

Sample codes	A_{3400} (cm^{-1})	A_{1630} (cm^{-1})	A_{1150} (cm^{-1})	A_{907} (cm^{-1})
G_1	29.96	0.80	23.37	2.88
X_1	37.94	1.00	48.28	4.89
PB_1	56.83	2.44	23.96	2.89
G_2	26.06	0.82	18.35	1.52
X_2	34.29	1.21	35.71	3.54
PB_2	53.17	2.55	19.58	1.53
G_3	36.31	0.77	22.70	1.86
X_3	47.17	1.02	31.96	2.54
PB_3	63.54	2.34	23.83	1.83
G_4	29.42	0.86	15.45	1.43
X_4	39.74	0.94	23.09	1.87
PB_4	56.44	2.57	16.82	1.45

PB_n – physical mixtures between G microparticles and xanthan (23/1, w/w).

monomers and the reaction mechanism proposed in Scheme 1 is correct.

- the peak areas at 3400 cm^{-1} for G microparticles are due to the opening of small amounts of epoxy groups of GMA;
- because the peak area values at 907 cm^{-1} (specific of epoxy vibrations) for X microparticles are increased compared to those for G microparticles and physical mixtures it can be concluded that the presence of xanthan gum in the reaction medium leads to the opening of a smaller number of epoxy groups;
- the higher value of peak area at 3400 cm^{-1} considering X microparticles is due to the presence of —OH groups from the molecule of xanthan.

3.2.2. Epoxy group content

The content of epoxy groups on the surface of microparticles was determined by tritimetric method namely HCl-dioxane method consisting in epoxy ring opening by HCl in a solution of dioxane, at room temperature (Vogel, 1958, Chapter XXXVIII). Also, the FT-IR spectroscopy allowed the determination of the GMA content in the copolymers on the basis of a calibration curve of monomeric standard solutions using the ratio between peak areas at 908 cm^{-1} (epoxy ring out of plane vibration) as indicative peak for GMA content and peak area at 1717 cm^{-1} (stretching peak of carbonyl groups) as reference peak. The GMA content in microparticles was determined by linear fit of the FT-IR experimental data and was expressed by the equations showed in Fig. 2.

The results of the epoxy group content determined by both methods are presented in Table 4.

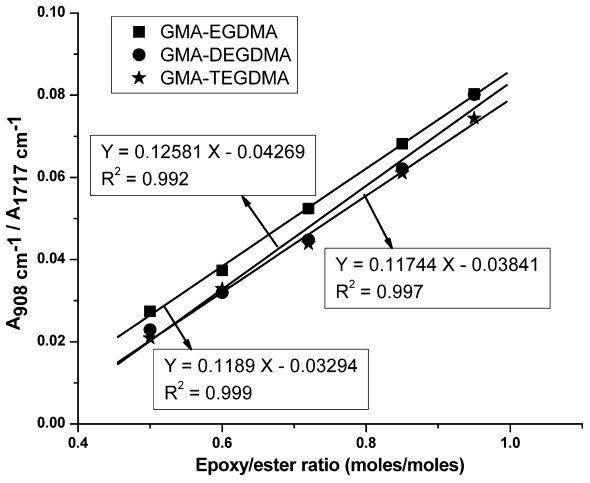

Fig. 2. Calibration curves of monomer standard solutions for GMA content determination by FT-IR spectroscopy.

Table 4
Epoxy group contents determined by titration and FT-IR analysis.

Sample codes	Epoxy group content (wt.%)		
	Theoretical	Titration	FT-IR
G_1	26.19	13.05	21.75
G_2	22. 43	13.29	19.13
G_3	25.43	15.17	20.89
G_4	24.72	7.51	15.89
X_1	25.10	20.89	23.12
X_2	21.49	19.51	20.90
X_3	24.37	22.27	23.81
X_4	23.69	9.84	18.48

The differences between the results obtained by both methods and theoretical values can be explained as follows:

1. By titration method only some part of epoxy groups are determined, especially those found on the surface of the microparticles. The small values registered by titration may be due to the fact that the majority of epoxy groups are masked by the complex crosslinked structures of the particles, which is obstructing the access of HCl though the mesh network. The small values may also be explained by the lower reactivity of the functional groups present in a crosslinked copolymer compared to the reactivity of the same groups present in a linear polymeric chain. In case of X microparticles it is observed that the values determined by titration are much closer to the calculated values. This is probably because the X microparticles show a higher swelling degree compared to G microparticles and thus the epoxy group contents can be determined also in the subsequent swollen domains.
2. G microparticles present a broad hydroxyl (—OH) band at 3400 cm^{-1} due to the ring opening reaction of some number of the epoxy groups. For this reason, in case of G microparticles the epoxy group content determined by FT-IR analysis is different from the theoretical value.

3.2.3. Particle sizes and porous structure

The particle size distribution of G and X microparticles is plotted in Fig. 3.

From Table 2 and Fig. 3 it can be seen that when xanthan is added to the reaction the microparticles exhibit a narrow size distribution and smaller average sizes.

To compare the difference that can occur in the morphological structure of G and X microparticles, the evolution of the synthesis process for both types of microparticles was investigated by SEM microscopy (Fig. 4).

From the early hours of the reaction the G_2 microparticles show a well-defined structure with good spherical shape and a broad particle size distribution whereas the X_2 microparticles present an agglomeration of spherical particles which disappears after 3 h from the beginning of the reaction because of the maturation of the beads. Finally, the X_2 microparticles have a spherical shape with a narrow particle size distribution. Also, the average diameter of X_2 microparticles is smaller than that of G_2 microparticles leading to the idea that xanthan has two roles: (1) as reactant alongside GMA and dimethacrylic monomers and (2) as suspension stabilizer in combination with PVA. Also, xanthan gum is commonly used as a stabilizer, emulsifier and thickener in food industry (Katzbauer, 1998; Sharma, Naresh, Dhuldhoya, Merchant, & Merchant, 2006).

The main factors determining the porous structure of microparticles are: monomer concentration, chemical nature of the monomers and type and concentration of porogenic agent. Pore volume, porosity, pore size distribution and surface area are the most important characteristics that define the porous nature (Malik & Ali, 2008; Malik et al., 2006; Talha Gokmen & Du Prez, 2012).

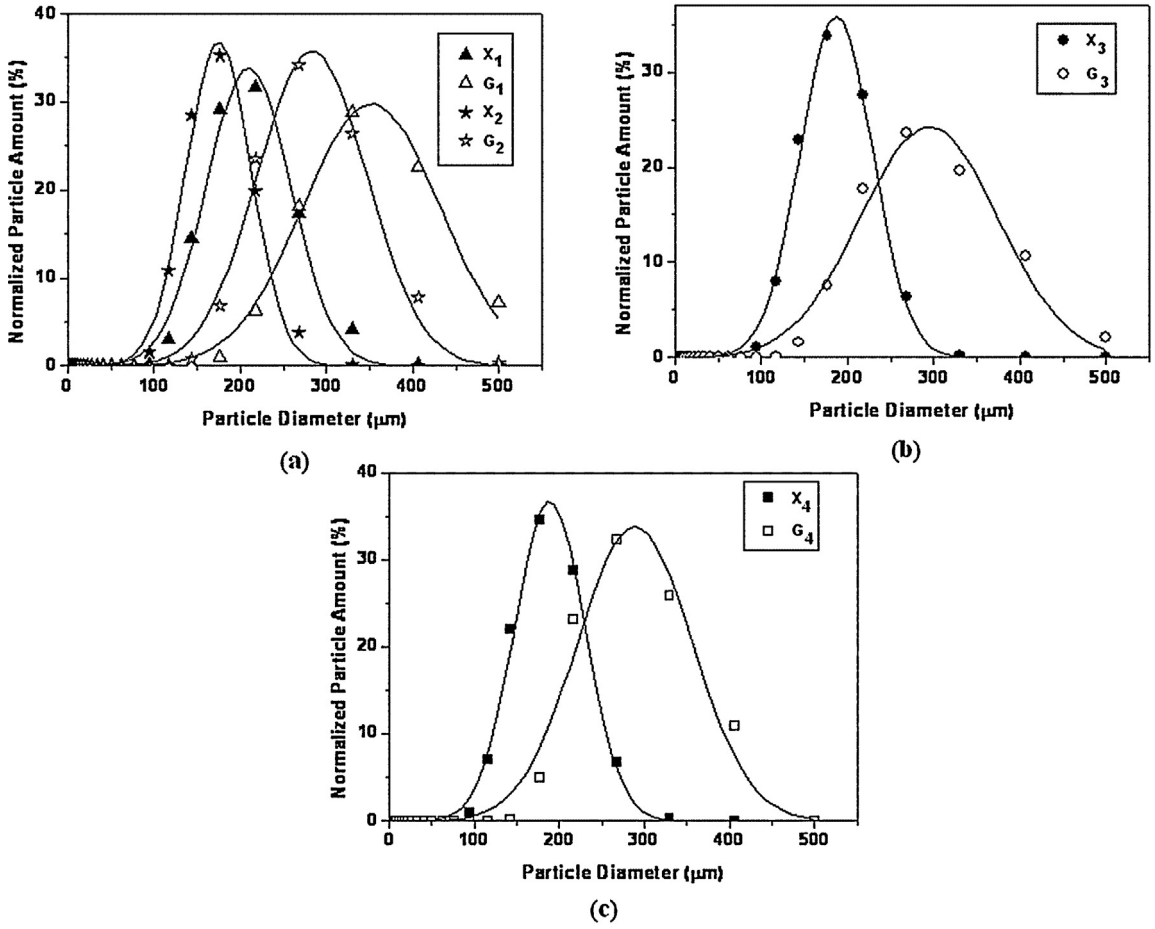

Fig. 3. Particle size distributions of G and X microparticles.

Table 5
Porosity parameters of G and X microparticles.

Sample codes	VP (mL/g)[a]	P (%)[a]	S_{BET} (m^2/g)[b]
G_1	0.598	44.32	69
G_3	0.524	41.01	49
G_4	0.450	35.28	31
X_1	0.425	35.63	129
X_3	0.233	22.37	50
X_4	0.176	17.68	44

[a] The pore volume and porosities were determined from skeletal and apparent densities.
[b] S_{BET} was determined using DVS method.

In Table 5 are listed the porous characteristics of G and X microparticles, such as the pore volume, porosity and the surface areas.

As seen from Table 5 depending on the nature of the dimethacrylic monomer the porosity values for G and X microparticles increase in the following order: $G_1 > G_3 > G_4$ and $X_1 > X_3 > X_4$, suggesting that a higher porous structure is obtained when dimethacrylic monomer has the shortest chain. This fact can be explained by the complexity of the crosslinking mechanism. This mechanism includes intra- and intermolecular reactions as well as the cyclization reactions that can appear in the early stage of the copolymerization reaction (Okay, 2000). In case of G and X microparticles the increase of the chain length of dimethacrylate ester leads to the increase of the number of cyclization and intramolecular reactions having as result the compaction of the copolymer chains and finally the decrease of porosity. In case of X microparticles the presence of xanthan contributes to the decrease of porosity and the increase of specific surface area values. The high values of the specific surface area for X microparticles can be explained by the fact that the X microparticles have more pores with smaller sizes compared to those for G microparticles.

3.2.4. Thermogravimetric analysis

The thermogravimetric characteristics and DTG curves for G and X microparticles are presented in Table 6 and Fig. 5, respectively.

The thermogravimetric analysis of xanthan (Sand, Yodav & Behari, 2010) and copolymers based on GMA (Jiang & Tu, 2010; Zulfiqar, Zulfiqar, Nawaz, McNeill, & Gorman, 1990) is well known in literature. Kinetic parameters such as activation energies and order of degradation reaction were calculated from TG curves using the Coats-Redfern method (Coats & Redfern, 1964).

The DTG curves for G and X micropaticles shows that they are thermally stable up to 180 °C and the microparticles present three stages of degradation. The temperature at which intensive degradation is observed was chosen as criterion to compare the thermal stability of microparticles. In the first stage of degradation (180–260 °C) was observed a mass loss ranging from 8.76% to 26.77% for G microparticles as well as from 5.57% to 14.77% for X microparticles. This mass loss can be attributed to the removal of various compounds such as: entrapped solvent or residual monomers that are incorporated in the pores of the microparticles. In the second stage of degradation (270–375 °C) a highest amount of mass loss was observed ranging from 58.21% to 75.82% for G microparticles and from 76.55% to 86.45% for X microparticles, respectively. In this stage the degradation probably starts at the ether linkage followed by random scission of the macromolecular chain. Also, from Table 6 it can be seen that in case of G

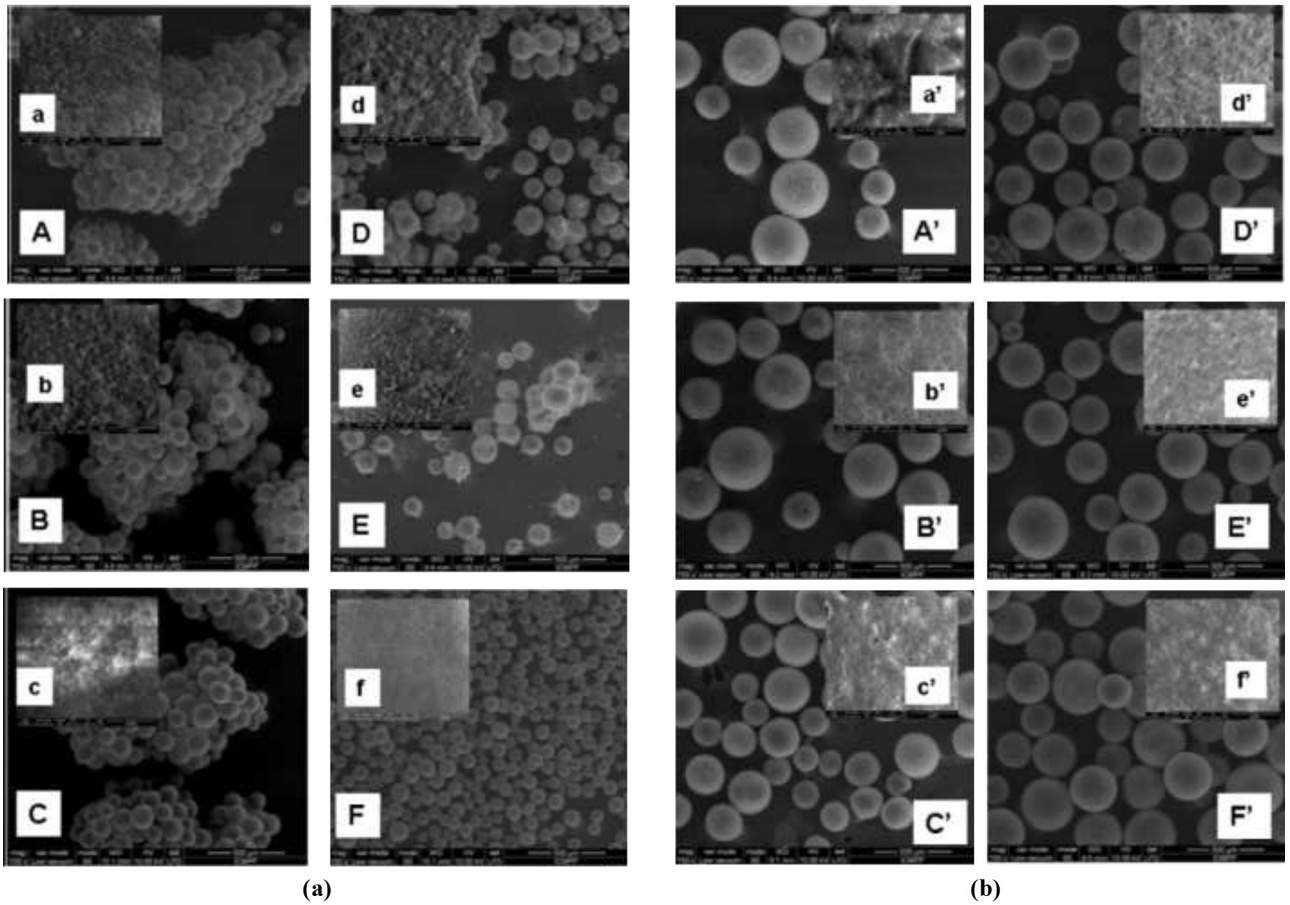

Fig. 4. SEM images of evolution of the synthesis process of the X_2 microparticles (a) and G_2 microparticles (b) [A, A′ – 1 h; B, B′ – 2 h; C, C′ – 3 h; D, D′ – 5 h; E, E′ – 7 h; F, F′ – 9 h].

Table 6
Thermogravimetric characteristics for Xan, G and X microparticles.

Samples codes	Decomposition temperature			Weight loss (%)	Residual mass (%)	E_a (kJ/mol)	n	R^2
	T_i (°C)	T_m (°C)	T_f (°C)					
	184	202	226	8.76		153	1.8	0.996
G_1	279	326	353	75.82	3.45	179	1.8	0.995
	353	412	435	11.97		210	1.8	0.993
	180	231	240	12.93		133	1.4	0.991
G_2	270	332	375	74.51	0.53	184	1.7	0.992
	380	416	460	12.03		425	2.6	0.994
	206	226	260	25		191	1.8	0.997
G_3	260	286	336	58.03	5.31	175	1.9	0.994
	336	386	435	11.66		171	1.8	0.991
	201	223	262	26.77		134	1.7	0.994
G_4	262	299	342	58.21	3.34	174	1.8	0.994
	342	389	427	11.68		187	1.8	0.992
	–	–	–	–		–	–	–
X_1	276	304	339	86.45	3.6	224	2	0.996
	339	403	428	9.95		185	1.8	0.992
	180	240	260	14.77		121	1.7	0.982
X_2	270	331	375	76.55	2.22	179	1.8	0.982
	380	411	431	6.46		327	1.3	0.998
	183	200	253	10.92		114	1.7	0.993
X_3	253	294	342	77.14	4.61	151	1.8	0.993
	342	396	426	7.33		181	1.8	0.992
	180	190	229	5.57		172	1.8	0.997
X_4	229	270	310	80.32	2.93	147	1.8	0.994
	310	384	417	11.18		143	1.7	0.990
	65	102	135	7.30		75	1.7	0.983
Xan	245	283	309	40.48	35.51	200	1.9	0.986
	309	411	510	16.71		61	1.1	0.989

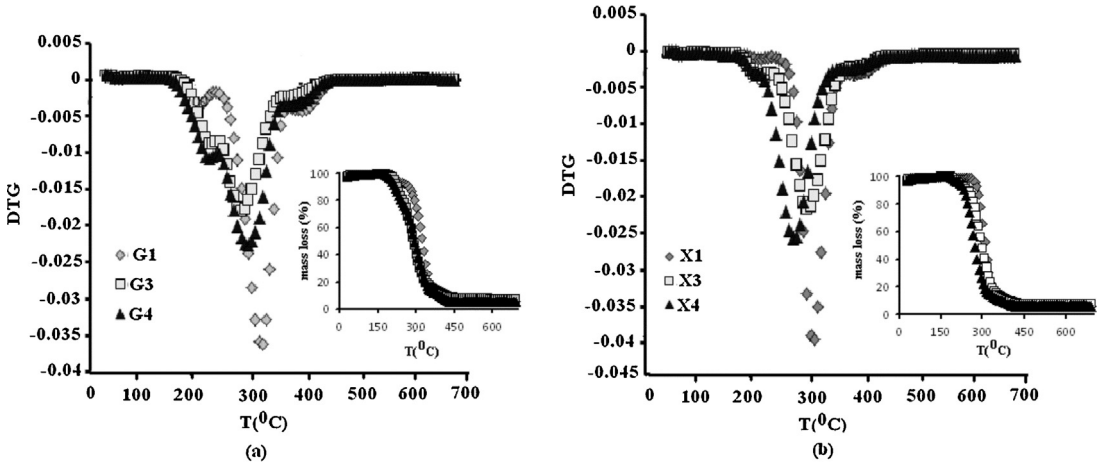

Fig. 5. DTG and TG curves for (a) G microparticles and (b) X microparticles.

microparticles the quantity and the chemical structure of the crosslinker has no influence on the activation energy values, probably due to the similar structure of the microparticles. In case of the X microparticles the degradation process occurs with distinct activation energies ranging from 224 kJ/mol for X_1 to 147 kJ/mol for X_4. These results can be an indication of the structural complexity of the microparticles. Also, the fractional values of the reaction order ranged from 1.3 to 2.6 suggest the complexity of the degradation process. Generally, the presence of xanthan in the structure of X microparticles slightly decreases the thermal stability of the microparticles.

3.2.5. Sorption–desorption isotherms

DVS is a rapid method for characterization of sorption/desorption isotherms of various materials. It is known from literature that the shape of sorption isotherms depends

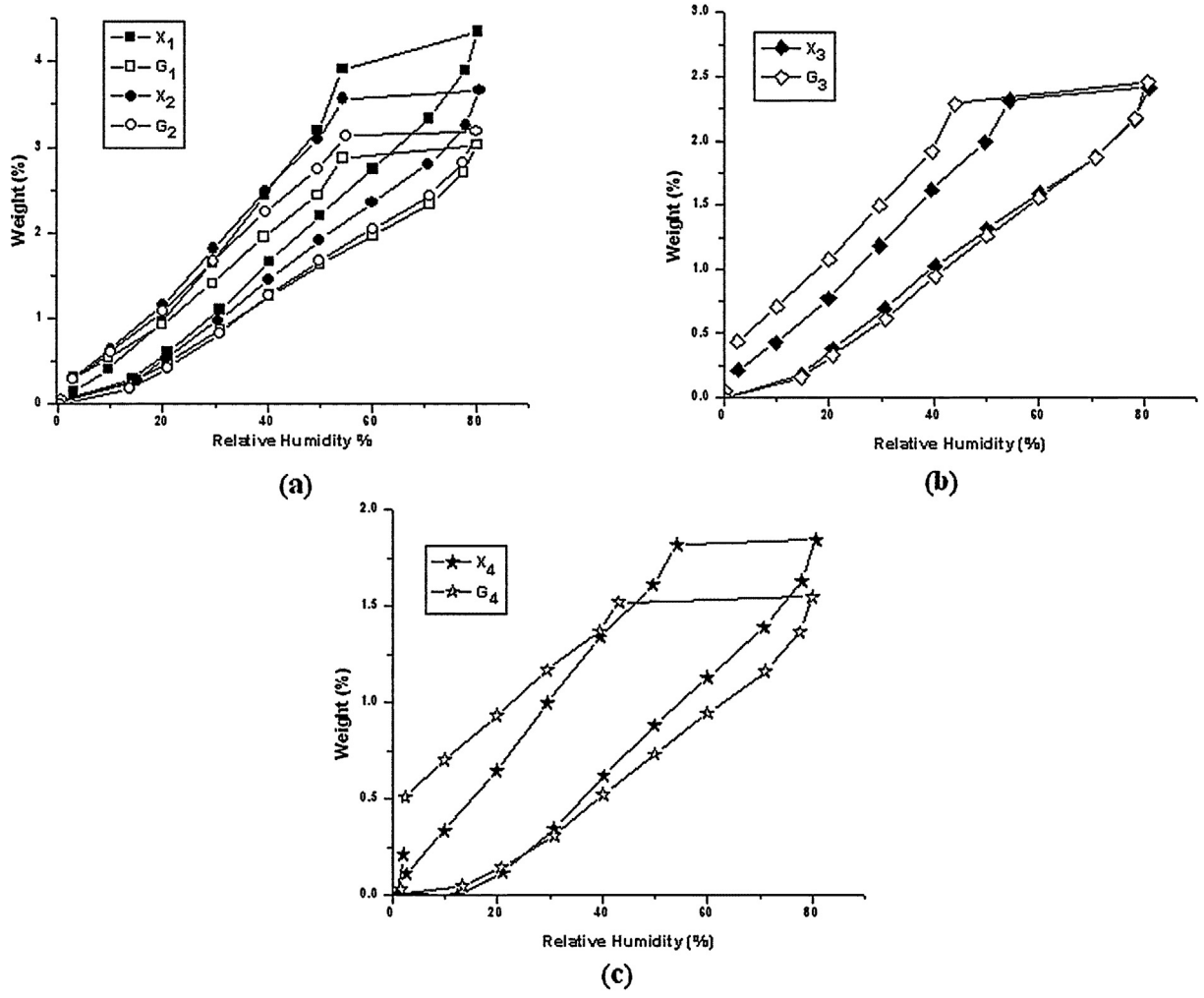

Fig. 6. Sorption and desorption isotherms for G and X microparticles determined by DVS method.

on the type, size and electronic structure of the studied material (Nistor, Stiubianu, Racles, & Cazacu, 2011). In our case the sorption/desorption isotherms were used to estimate the specific surface areas (Table 4) as well as to provide information about the porous structure of the microparticles. The BET kinetic model is often used for modeling the sorption isotherms. This model is based on the following equation:

$$W = \frac{W_m \cdot C \cdot RH}{(1 - RH) \cdot (1 - RH + C \cdot RH)} \quad (3)$$

where W is the weight of sorbed water, W_m the weight of water forming a monolayer, C is the sorption constant, RH – relative humidity.

BET model describes the sorption isotherms up to a relative humidity of 40%, depending on the type of sorption isotherm and the type of material (Ng & Mintova, 2008).

The sorption and desorption isotherms performed at 25 °C for G and X microparticles are presented in Fig. 6.

According to IUPAC classification, the sorption/desorption isotherms can be associated to type V curves that is characteristic to the sorption on hydrophobic/low hydrophilic materials with weak sorbent–water interactions and with low sorption at low RH (Ng & Mintova, 2008). This type of sorption isotherms is characteristic for porous materials and show hysteresis loop between sorption and desorption cycles in low and medium humidity levels. The adsorption hysteresis is H_2 type and is characteristic to the systems where the pores are interconnected and the distribution of pore size and pore structure are more complex and is not well-defined (Mason, 1982).

From Fig. 6 it is observed that the X microparticles present higher water vapor sorption capacity as compared with G microparticles. This behavior can be explained by the difference in their structure and morphology as well as by the presence in the structure of X microparticles of xanthan that is a hydrophilic polymer.

4. Conclusions

In this study porous microparticles based on GMA, dimethacrylic monomers (EGDMA, DEGDMA, TEGDMA) and XAN were prepared by a simple and efficient method namely suspension polymerization technique.

The presence of xanthan in the structure of X microparticles leads to the preparation of the complex microparticulate systems that are characterized by the high content of epoxy groups, smaller sizes, high values of the specific surface areas and better sorption capacities compared to those based on GMA and dimethacrylic monomers.

Due to their properties X microparticles can be used in various applications, more precisely for the retention, delivery and controlled release of various drugs as well as in biotechnological field as polymeric supports for enzyme immobilization.

References

Bakhshi, H., Zohuriaan-Mehr, M. J., Bouhendi, H., & Kabiri, K. (2009). Spectral and chemical determination of copolymer composition of poly(butyl acrylate-*co*-glycidyl methacrylate) from emulsion polymerization. *Polymer Testing*, *28*, 730–736.

Bencina, M., Bencina, K., Stancar, A., & Podgornik, A. (2005). Immobilization of deoxyribonuclease via epoxy groups of methacrylate monoliths: Use of deoxyribonuclease bioreactor in reverse transcription-polymerase chain reaction. *Journal of Chromatography A*, *1065*, 83–91.

Brooks, B. (2010). Suspension polymerization processes. *Chemical Engineering & Technology*, *33*, 1737–1744.

Canto, L. B., & Pessan, L. A. (2002). Determination of the composition of styrene-glycidyl methacrylate copolymers by FTIR and titration. *Polymer Testing*, *21*, 35–38.

Coats, A. W., & Redfern, J. P. (1964). Kinetic parameters from thermogravimetric data. *Nature*, *201*, 68–69.

Danquah, M. K., Ho, J., & Forde, G. M. (2007). Performance of R-N-(R′)-R″-functionalized poly(glycidyl methacrylate-*co*-ethylene glycol dimethacrylate) monolithic sorbent for plasmid DNA adsorption. *Journal of Separation Science*, *30*, 2843–2850.

Jiang, X., & Tu, W. (2010). Stable poly(glycidyl methacrylate-*co*-ethylene glycol dimethacrylate) microspheres via precipitation polymerization. *Journal of Applied Polymer Science*, *115*, 963–968.

Jin, J. M., Lee, J. M., Ha, M. H., Lee, K., & Choe, S. (2007). Highly crosslinked poly(glycidyl methacrylate-*co*-divinyl benzene) particles by precipitation polymerization. *Polymer*, *48*, 3107–3115.

Katzbauer, B. (1998). Properties and applications of xanthan gum. *Polymer Degradation and Stability*, *59*, 81–84.

Kim, J. W., & Suh, K. D. (2008). Monodisperse polymer particles synthesized by seeded polymerization techniques. *Journal of Industrial and Engineering Chemistry*, *14*, 1–9.

Malik, M. A., & Ali, S. W. (2008). Synthesis and simple method of estimating macroporosity of methyl methacrylate-divinylbenzene copolymer beads. *Journal of Applied Polymer Science*, *109*, 3817–3824.

Malik, M. A., Ali, S. N., & Waseem, S. (2006). A simple method for estimating parameters representing macroporosity of porous styrene-divinylbenzene copolymers. *Journal of Applied Polymer Science*, *99*, 3565–3570.

Malovic, L., Nastovic, A., Sandic, Z., Markovik, J., Dordevic, D., & Vukovic, Z. (2007). Surface modification of macroporous glycidyl methacrylate based copolymers for selective sorption of heavy metals. *Journal of Material Science*, *42*, 3326–3337.

Marinovic, S., Vukovic, Z., Nastasovic, A., Milutinovic-Nikolic, A., & Jovanovic, D. (2011). Poly(glycidyl methacrylate-*co*-ethylene glycol dimethacrylate)/clay composite. *Materials Chemistry and Physics*, *128*, 291–297.

Mason, G. (1982). The effect of pore space connectivity on the hysteresis of capillary condensation in adsorption/desorption isotherms. *Journal of Colloid and Interface Science*, *88*, 36–46.

Miletic, N., Rohandi, R., Vukovic, Z., Nastasovic, A., & Loos, K. (2009). Surface modification of macroporous poly(glycidyl methacrylate-*co*-ethylene glycol dimethacrylate) resins for improved *Candida antartica lipase B* immobilization. *Reactive and Functional Polymers*, *69*, 68–75.

Milosavic, N., Prodanovic, R., Jovanovic, S., & Vujcic, Z. (2007). Immobilization of glucoamylase via its carbohydrate moiety on macroporous poly(GMA-*co*-EGDMA). *Enzyme and Microbial Technology*, *40*, 1422–1426.

Nistor, A., Stiubianu, G., Racles, C., & Cazacu, M. (2011). Evaluation of the water sorption capacity of some polymeric materials by dynamic vapour sorption. *Materiale Plastice*, *45*, 33–37.

Ng, E. P., & Mintova, S. (2008). Nanoporous materials with enhanced hydrophilicity and high water sorption capacity. *Microporous and Mesoporous Materials*, *114*, 1–26.

Okay, O. (2000). Macroporous copolymer networks. *Progress in Polymer Science*, *25*, 711–779.

Qi, T., Sonoda, A., Makita, Y., Kanoh, H., Ooi, K., & Hirotsu, T. (2002). Porous properties of poly(glycidyl methacrylate-*co*-trimethyl propane trimethacrylate) resins synthesized by suspension polymerization. *Journal of Applied Polymer Science*, *83*, 2374–2381.

Rahman, A., Iqbal, M., Rahman, F., Fu, D., Yaseen, M., Lv, Y., et al. (2012). Synthesis and characterization of reactive macroporous poly(glycidyl methacrylate–triallyl isocyanurate–ethylene glycol dimethacrylate) microspheres by suspension polymerization. Effect of synthesis variables on surface area and porosity. *Journal of Applied Polymer Science*, *124*, 915–926.

Sand, A., Yadav, M., & Behari, K. (2010). Graft copolymerization of 2-acrylamidoglycolic acid onto xanthan gum and study of its physicochemical properties. *Carbohydrate Polymers*, *81*, 626–632.

Seidl, J., Malinsky, J., Dusek, K., & Heitz, W. (1967). Macroporous styrene-divinylbenzene copolymers and their application in chromatography and for preparation of ion exchange resins. *Advances in Polymer Science*, *5*, 113–213.

Senkal, B. F., & Yavuz, E. (2006). Crosslinked poly(glycidyl methacrylate)-based resin for removal of mercury from aqueous solutions. *Journal of Applied Polymer Science*, *101*, 348–352.

Sharma, B. R., Naresh, L., Dhuldhoya, N. C., Merchant, S. U., & Merchant, U. C. (2006). Xanthan gum – a boon to food industry. *Food Promotion Chronicle*, *1*, 27–30.

Svec, F., Hradil, J., Coupek, J., & Kalal, J. (1975). Reactive polymers I. Macroporous methacrylate copolymers containing epoxy groups. *Die Angewandte Makromolekulare Chemie*, *48*, 135–143.

Talha Gokmen, M., & Du Prez, F. E. (2012). Porous polymer particles – a comprehensive guide to synthesis, characterization, functionalization and applications. *Progress in Polymer Science*, *37*, 365–405.

Vaidya, B. K., Ingavle, G. C., Ponrathnam, S., Kulkarni, B. D., & Nene, S. N. (2008). Immobilization of *Candida rugosa* lipase on poly(allyl glycidyl ether-*co*-ethylene glycol dimethacrylate) macroporous polymer particles. *Bioresource Technology*, *99*, 3623–3629.

Vasiliu, S., Bunia, I., & Neagu, V. (2009). Core–shell microparticles based on acrylic ion exchange resin/polysaccharides as drug carriers. *Ion Exchange Letters*, *2*, 27–30.

Vasiliu, S., Bunia, I., Racovita, S., & Neagu, V. (2011). Adsorption of cefotaxime sodium salt on polymer coated ion exchange resin microparticles: Kinetics, equilibrium and thermodynamic studies. *Carbohydrate Polymers*, *85*, 376–387.

Vivaldo-Lima, E., Wood, P. E., Hamielec, A. E., & Penlidis, A. (1997). An update review on suspension polymerization. *Industrial & Engineering Chemistry Research*, *36*, 939–965.

Vlad, C. D., & Vasiliu, S. (2010). Crosslinking polymerization of polyfunctional monomers by free radical mechanism. *Polimery*, *55*, 181–185.

Vogel, A. I. (1958). *Elemental practical organic chemistry. Part III. Quantitative organic analysis*. London: Longman Group Limited.

Wang, R., Zhang, Y., Ma, G., & Su, Z. (2006). Preparation of uniform poly(glycidyl methacrylate) porous microspheres by membrane emulsification polymerization technology. *Journal of Applied Polymer Science*, *102*, 5018–5027.

Zhou, W. Q., Gu, T. Y., Su, Z. G., & Ma, G. H. (2007). Synthesis of macroporous poly(glycidyl methacrylate) microspheres by surfactant reverse micelles swelling method. *European Polymer Journal*, *43*, 4493–4502.

Zulfiqar, S., Zulfiqar, M., Nawaz, M., McNeill, I. C., & Gorman, J. G. (1990). Thermal degradation of poly(glycidyl methacrylate). *Polymer Degradation and Stability*, *30*, 195–203.